Original Article | Journal of Biosystems Engineering

J. Biosyst. Eng. 43(2):138-147. (2018. 6)
https://doi.org/10.5307/JBE.2018.43.2.138

eISSN : 2234-1862
pISSN : 1738-1266

Yield Prediction of Chinese Cabbage (*Brassicaceae*) Using Broadband Multispectral Imagery Mounted Unmanned Aerial System in the Air and Narrowband Hyperspectral Imagery on the Ground

Ye Seong Kang[1,2], Chan Seok Ryu[1,2]*, Seong Heon Kim[1,2], Sae Rom Jun[1,2], Si Hyeong Jang[1,2], Jun Woo Park[1,2], Tapash Kumar Sarkar[1,2], Hye young Song[1,2]

[1]*Division of Bio-System Engineering, Gyeongsang National University, Jinju, Republic of Korea*
[2]*Institute of Agriculture & Life Science, Gyeongsang National University, Jinju, Republic of Korea*

Received: March 3th, 2018; Revised: May 21th, 2018; Accepted: May 25th, 2018

Abstract

Purpose: A narrowband hyperspectral imaging sensor of high-dimensional spectral bands is advantageous for identifying the reflectance by selecting the significant spectral bands for predicting crop yield over the broadband multispectral imaging sensor for each wavelength range of the crop canopy. The images acquired by each imaging sensor were used to develop the models for predicting the Chinese cabbage yield. **Methods:** The models for predicting the Chinese cabbage (*Brassica campestris L.*) yield, with multispectral images based on unmanned aerial vehicle (UAV), were developed by simple linear regression (SLR) using vegetation indices, and forward stepwise multiple linear regression (MLR) using four spectral bands. The model with hyperspectral images based on the ground were developed using forward stepwise MLR from the significant spectral bands selected by dimension reduction methods based on a partial least squares regression (PLSR) model of high precision and accuracy. **Results:** The SLR model by the multispectral image cannot predict the yield well because of its low sensitivity in high fresh weight. Despite improved sensitivity in high fresh weight of the MLR model, its precision and accuracy was unsuitable for predicting the yield as its R^2 is 0.697, root-mean-square error (RMSE) is 1170 g/plant, relative error (RE) is 67.1%. When selecting the significant spectral bands for predicting the yield using hyperspectral images, the MLR model using four spectral bands show high precision and accuracy, with 0.891 for R^2, 616 g/plant for the RMSE, and 35.3% for the RE. **Conclusions:** Little difference was observed in the precision and accuracy of the PLSR model of 0.896 for R^2, 576.7 g/plant for the RMSE, and 33.1% for the RE, compared with the MLR model. If the multispectral imaging sensor composed of the significant spectral bands is produced, the crop yield of a wide area can be predicted using a UAV.

Keywords: Chinese cabbage, hyperspectral image, linear regression model, multispectral image, UAV

Introduction

Monitoring the growth status of crops is one of the methods for archiving productivity improvement and stable cultivation. Traditionally, it is being monitored from seeding to harvest based on the farmer's experience. In other words, it is meaning that it is difficult and risk to approach cultivating other crops without the experience. Therefore, the growth status of the crops needs to be assessed by the value of its canopy sensed by an imaging sensor to facilitate an objective judgment without requiring experience on various crop cultivations. Various reflectances of the canopy can be obtained by multispectral or hyperspectral imaging sensors (Zarco-Tejada et al., 2013). The reflectances of the crop's canopy are different between the near-infrared (NIR) band and visible bands. The reflectance in the NIR band is high as a result of the spongy parenchyma effect inside a healthy canopy, thereby aggravating the reflectance of many leaf layers.

***Corresponding author:** Chan Seok Ryu
Tel: +82-55-772-1897; **Fax:** +82-55-772-1898
E-mail: ryucs@gnu.ac.kr

The visible bands are related to the radiation absorbed by the crop pigments inside the palisade parenchyma and vary with the wavelength of the incident radiation. The contrast between bands is used to calculate various vegetation indices (Kang et al., 2017). The indices are compared with the crop traits, including the leaf area index (LAI), leaf chlorophyll, and yield prediction using simple linear regression analysis and are important indicators to monitor the crops (Liu et al., 2017). Particularly, the normalized difference vegetation index (NDVI) and simple ratio (SR) are the most widely used. However, the NDVI easily saturates in a healthy vegetation canopy. The saturation inhibits the reflectance sensitivity in the red band owing to the high absorption coefficient of chlorophyll in the canopy (Nguy-Robertson et al., 2012). Further, the saturation is attributed to the NDVI formula by the high NIR band reflected by the canopy. It is prone to scattering on the vegetation canopy of healthy growth. The SRs calculated by the red edge and visible bands might be alternatives to overcome the limitation (Kang et al., 2017). The SR was used to predict a large-area rice yield with the SR reflected canopy at the booting stage using multispectral bands of satellite imagery (Wang et al., 2010). Additionally, the rice green LAI (gLAI) of crop canopies was retrieved from the spectral indices and the SR calculated by the bands of hyperspectral imagery from satellites (Haboudane et al., 2004). Further, various vegetation indices of crop canopies were evaluated to retrieve the gLAI of the crops (Viña et al., 2011).

Hence, remote sensing technology carrying various imaging sensors has great potential because it enables wide-area and real-time acquisition for sensing crop conditions (Ryu et al., 2011). The technology contains some information such as remote sensing platform, global positioning system (GPS), and geographic information system (GIS) for investigating spatial variability (Huang et al., 2016). Traditional remote sensing platforms such as artificial satellites and aircraft are not suitable for proximal remote sensing for precisely monitoring the growth status because of their low spatial and temporal resolutions (Mulla, 2013). Recently, small unmanned aerial vehicles (UAVs) have been reported to fly at low altitudes, which have been achieved by the powerful platform for precisely monitoring the growth status of the detected individual crop as high spatial resolution. Further, it is beneficial in terms of unconstrained scheduling, low price, low-altitude flying, and safer than a piloted aircraft (Kang et al., 2016). The multispectral imaging sensors, commonly equipped with a UAV, cannot easily predict the physiological attributes of different crops. Therefore, it is essential to select key spectral bands using high-dimensional data in crop canopies extracted by the hyperspectral images for optimally predicting the physiological attributes of different crops. The high-dimensional data have been handled by some spectral band selection methods because of the high correlation inherent in adjacent spectral bands. Most spectral band selection methods were conducted using partial least squares regression (PLSR) and multiple linear regression (MLR) with stepwise discriminant analysis (Song et al., 2011). PLSR is a powerful tool to predict physiological attributes; however, it has some drawbacks because of the threshold selection of variables to be included in PLSR associated with the process of choosing the latent factors (Martinez et al., 2017). Nevertheless, the weight value and variable importance for projection (VIP) can be used to determine the important variables (Stellacci et al., 2016). MLR with stepwise discriminant analysis provides the best linear spectral combinations to assess physiological attributes. The methods can be extremely useful to provide data interpretation or multispectral imaging sensor development. The growth models developed by such linear regression analysis methods have been used to simulate the crop growth status. The models are useful in predicting crop yields before harvest to allow decision making in crop yield management (Jin et al., 2018).

In recent studies, the unmanned aerial system had been utilized to assess the nutritional status in maize (Gabriel et al., 2017) and monitor wheat growth (Mengmeng et al., 2017) from multispectral imagery. Further, grain yield had been predicted using the system to monitor the dry matter yield of triticale (Noack, 2016), and the biomass and grain yield of rice by the NDVI (Swain et al., 2010; Teoh et al., 2016; Zhou et al., 2017). The chlorophyll in oat was predicted using relevance vector machines coupled with cross-validation and backward elimination from thermal and multispectral imagery (Elarab et al., 2015). Multivariate analyses such as partial least squares regression and least squares-support vector machine with spectral pre- processing using multiplicative scatter correction and standard normal variable was performed to predict carbon and nitrogen contents in citrus canopy from hyperspectral

imagery (Xuefeng et al., 2016).

The objectives of this study are to develop the models with spectral bands selection for predicting the yield of autumn Chinese cabbage (*Brassica campestris L.*), with some spectral bands in remotely sensed canopies by multispectral imaging sensor equipped with a fixed-wing UAV, and canopy sensing by hyperspectral imaging sensor based on the ground, depending on the vegetation stages of the Chinese cabbage planted on the different dates during the growing seasons in 2015.

Materials and Methods

Field experiment

The study was conducted at Heaje-myeon (35° 4`11.28`` N, 126° 18`21.25`` E, approximately 63 m above sea levels) in 2015. The plot at Haeje-myeon is a silty clay loam of alkaline and low stone content. The average annual temperature and rainfall at the area were 13.4°C and 948.6 mm, respectively, in 2015. The plots comprised a design with the different planting dates such as normal plating (7th Sept.), one-week-delay planting (19th Sept.), and two-week-delay planting (25th Sept.) with three replications. The variety used for the experiment was Chinese cabbage (Whistle, Sakata Korea Co., Ltd., Rep. Korea) that is suitable to cultivate in the autumn.

Image acquisition

A multispectral image sensor, Multispec-4c (Sensefly Ltd., Sheseaux-Lausanne, Switzerland), shown in Figure 1 (a), equipped with an upward-facing sunshine sensor to correct the reflectance data in each band between the multitemporal images irrespective of light conditions, was mounted on the fixed-wing UAV to collect the images of the crop canopy. The camera and sunshine sensor of the imaging sensor was configured to measure the reflectance value of the central wavelength and full width at half maximum (FWHM) at green (550 ± 40 nm), red (660 ± 40 nm), red edge (735 ± 10 nm), and NIR (790 ± 40 nm) to meet the requirements of the monitoring application. The full scene size of each band image was provided as a 1.2-megapixel image in the raw format with a spatial resolution of 6 cm/pixel at approximately 50 m. Autonomous flights were conducted with an interval of approximately one week on 7th Oct., 21st Oct., and 4th Nov. in 2015 from the early growth stage to harvest. The images were acquired during midday to reduce the influence of incident light angle and dew on the leaf surface owing to the clear sky (Onoyama et al., 2013).

As shown in Figure 1 (b), the platform consisted of a 0.96-m wingspan fixed-wing UAV capable of a 50-min endurance at maximum with 0.69 kg take-off weight and a ground speed of approximately 10 m/s (eBee, Sensefly, Switzerland). The platform was operated by an autopilot associated with autonomous flight (eBee, senseFly, Cheseaux-Lausanne, Switzerland) based on a differential GPS (DGPS), three- axis accelerometer, gyros, and a three-axis magnetometer. The artificial intelligence inside the autopilot continuously analyzes the onboard inertial measurement unit and GPS data to control and optimize every aspect of the flight. The flight plan software (eMotion, senseFly, Cheseaux-Lausanne, Switzerland) on the ground and the UAV were connected through a radio link where the position, altitude, and status data were transmitted at a 2.3 GHz frequency within approximately a 3 km range.

(a) (b)

Figure 1. Multispectral image sensor (Multispec-4c) (a), Unmanned aerial vehicle (eBee) (b)

Figure 2. Hyperspectral image sensor (VNIR PS)

A hyperspectral image sensor, i.e., the VNIR spectral imaging sensor (PS, Spectral Imaging Ltd., Oulu, Finland) as shown in Figure 2, was operated to collect the images of the Chinese cabbage canopy on the ground. The images of the sensor are acquired by the scanner method based on the push broom. The spectral resolution of the images is 2.8 nm and comprises 519 spectral bands in the wavelength range of 400–1000 nm. The hyperspectral images were acquired at the same date as the multispectral images and at ~2 m height with an 18% reference board for light correction.

Image processing

The plurality of images per flight was acquired based on the flight plan software (eMotion, Sensefly Ltd., Sheseaux-Lausanne, Switzerland) using the information from the gyro and GPS. The mosaicking images considering each band was obtained using a UAV mapping software (Pix4D mapper pro, Pix4D, Lausanne, Switzerland), and tagged image file format of 8 bit/pixel images were produced. The coordinates of some targets were measured as the ground control points (GCPs) maintained throughout the vegetation stages with an RTK-GPS (V30 SNSS RTK System, Hi-Target Surveying Instrument Co. Ltd., China) to georeferenced images through a quadratic equation with the UAV mapping software using GCPs.

The single NIR band or SR calculated by the NIR and visible bands were used to separate the vegetation area of the canopies based on Ortho's threshold method using an image processing software (ENVI 4.7, Harris Geospatial Solutions Inc., Broomfield, CO. USA). Each sampling area was fixed as the region of interest as shown in Figure 3.

Modeling methods

Several vegetation indices (VIs) were chosen for the model of fresh weight as shown in Table 1. SLR and MLR

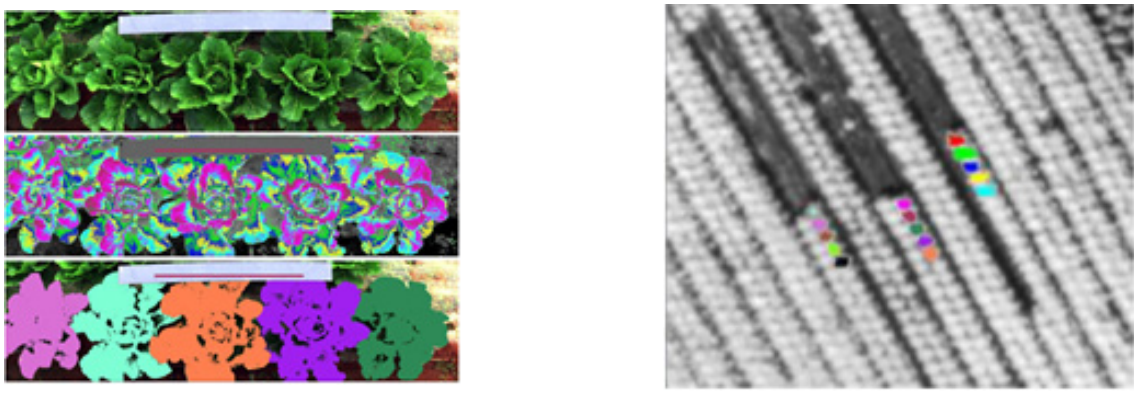

(a) (b)

Figure 3. Extraction of canopy areas in hyperspectral image (a) and multispectral image (b)

Table 1. Formula of vegetation indices

Vegetation indices	Formula	Reference
NDVI	DN_{nir} - DN_{red}/ DN_{nir} + DN_{red}	Rouse et al., 1974
GreenNDVI	DN_{nir} - DN_{green}/ DN_{nir} + DN_{green}	Gitelson et al., 1996
Red edge NDVI	$DN_{red\ edge}$ – DN_{red}/ $DN_{red\ edge}$ + DN_{red}	Sharma et al., 2015
Red edge GreenNDVI	$DN_{red\ edge}$ – DN_{green}/ $DN_{red\ edge}$ + DN_{green}	Kang et al., 2017
Simple ratio	$DN_{nir\ or\ red\ edge}$/ $DN_{visible\ ratio}$	Jordan., 1969

were computed to analyze the relationship between the fresh weight of Chinese cabbage and the VIs using the spectral bands of the canopies.

To reduce the high-dimensional spectral bands of canopies sensed in the hyperspectral images, the weight value and VIP based on PLSR were measured by the R project (version 3.2.3, R Foundation for Statistical Computing, Vienna, Austria). The forward stepwise multiple linear modeling for reducing the number of spectral bands was computed using SPSS (ver. 24, IBM SPSS Statistics, IBM Corp., Armonk, NY, USA). The coefficient of determination (R^2) and the root-mean-square error (RMSE) were used to evaluate the performance of the simple and MLR models.

Results and Discussion

Modeling of fresh weight for Chinese cabbage by multispectral image

A total of 59 samples out of 60 samples were used because the location of one sample in the image was not identified. The mean value of fresh weight for Chinese cabbage was 1743 g/plant and the standard deviation was 1784 g/plant for all samples. The SLR models of fresh weight for Chinese cabbage using VIs with all data of all growth stages are presented in Table 2. The R^2 values of all models are less than 0.397, their RMSE values exceed 1410 g/plant, and their RE values exceed 80%. This means that the fresh weight of Chinese cabbage is difficult to predict using VIs because of the low accuracy and precision of the VI models as shown in Figure 4 (a).

The forward stepwise MLR models of fresh weight for Chinese cabbage using multispectral bands with all growth stage data are presented in Table 3. The precision and accuracy of the MLR models are increased compared with those of the SLR models. The most suitable MLR model is established with four bands and its precision and accuracy are 0.607, 1170 g/plant and 67.1%, respectively. Despite the sensitivity improvement at the high fresh weight as shown in Figure 4 (b), the fresh

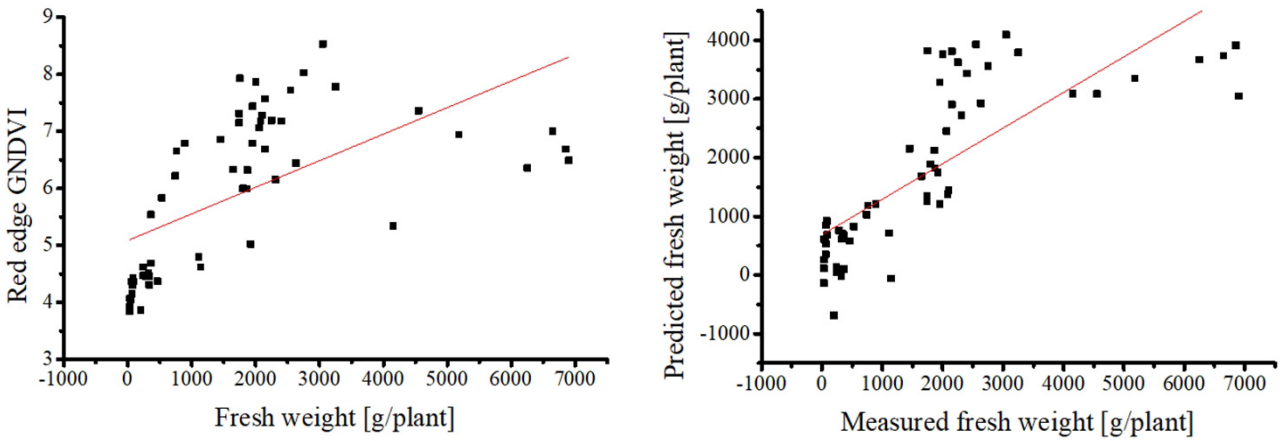

(a) (b)

Figure 4. Simple linear regression graph for predicting fresh weight using red edge GNDVI (a), MLR graph for predicting fresh weight using four spectral bands (b)

Table 2. Simple linear regression model of fresh weight for Chinese cabbage using vegetation indices

Vegetation indices	Equation	R^2 (n=59)	RMSE [g/plant]	RE [%]
NDVI	14530*x*-11069	0.214	1609	92.3
GNDVI	15025*x*-10223	0.181	1643	94.3
Red edge NDVI	12439*x*-8477.4	0.298	1521	87.3
Red edge GNDVI	17930*x*-10790	0.397	1410	80.9
NIR/Red	67.09*x*+400.7	0.114	1708	98.0
NIR/Green	256.6*x*-692.7	0.138	1685	96.7
Red edge/Red	140.9*x*-22.46	0.196	1627	93.3
Red edge/Green	789.5*x*-2937	0.369	1442	82.7

x, Values in each vegetation indices

weight of Chinese cabbage was difficult to predict accurately because the RMSE exceeded 1 kg/plant and the relative error exceeded 65%.

Modeling of fresh weight for Chinese cabbage by hyperspectral images

The PLSR model of fresh weight for Chinese cabbage using hyperspectral bands with all growth stage data is presented in Table 4. The latent variable was determined as six by predicting the residual error sum of squares statistics in the PLSR (Li et al., 2002). The fresh weight of Chinese cabbage was predicted as 0.896 for R^2, 576.7 g/plant for the RMSE, and 33.1% for the RE. The model precision increased by approximately 30% and the accuracy also improved by more than 50% compared with those of the forward stepwise MLR model with four bands. The precision and accuracy of the validation model based on leave one out was 0.848 for R^2, 696.3 g/plant for the RMSE, and 40% for the RE. The variation in reflectance depending on all the wavelengths and the PLSR model of fresh weight for Chinese cabbage are presented in Figure 5. The fresh weight of Chinese cabbage can be predicted using the PLSR model. However, it requires the information of full spectral bands for a high

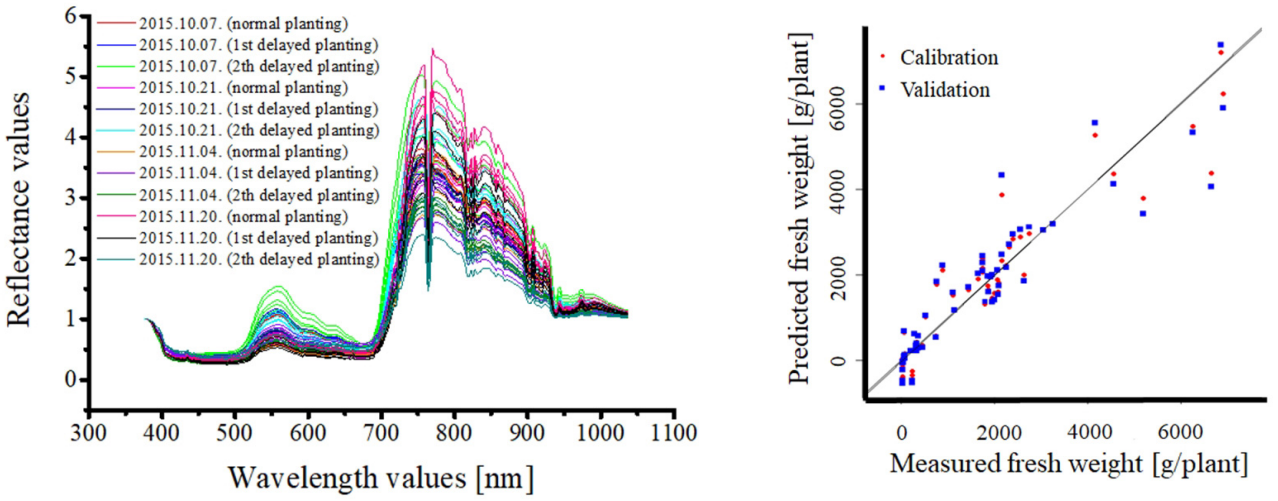

(a) (b)

Figure 5. Reflectance value of canopies in hyperspectral images (a), partial least squares regression model graph for predicting fresh weight using 519 spectral bands (b)

Table 3. MLR model of fresh weight for Chinese cabbage by forward stepwise method

Selected spectral bands	Equation	R^2 (n=59)	RMSE [g/plant]	RE [%]
Red, Red edge	$13309x_1$-$57065x_2$-1125.1	0.457	1349	77.4
Red, Red edge, Green	$-117810x_1$+$22421x_2$+$45377x_3$-520.88	0.547	1244	71.4
Red, Red edge, Green, NIR	$-5866.1x_1$-$131165x_2$+$31342x_3$+$56489x_4$+93.673	0.607	1170	67.1

Reflectance values in x_1, Red; x_2, Red edge; x_3, Green; x_4, NIR

Table 4. Partial least squares regression model of fresh weight for Chinese cabbage

		Fresh weight (n=59)
LV		6
Calibration	R^2	0.896
	RMSE [g/plant]	576.7
	RE [%]	33.1
Validation	R^2	0.848
	RMSE [g/plant]	696.3
	RE [%]	40.0

performance. Therefore, the significant spectral bands were selected by the stepwise method to reduce the number of spectral bands in the model while maintaining the model performance.

The spectral bands were reduced by selecting the peak points between each maximum and minimum weight value of 10 points within each spectral bandwidth (blue, green, red, red edge, NIR) and the bands with the value of VIP of more than 1.2 remained after the dimension reduction, as shown in Figure 6. Based on this method, 98 bands out of 519 bands were selected as the significant spectral bands.

Finally, a forward stepwise MLR using 98 bands was applied to select the spectral band for predicting the fresh weight of Chinese cabbage. The maximum number of bands for forward stepwise MLR was limited to five bands for commercializing the spectral imaging sensor. The precision and accuracy of the models using the selected spectral bands are shown in Table 5. The five selected spectral bands are in order of green (559.6 nm), red edge (768.8 nm), green (590.9 nm), red edge (723.8 nm), and red edge (721.3 nm), respectively. Although the precision and accuracy of the model with five bands was the best with 0.898 for R^2, 602 g/plant for the RMSE, and 34.5% for the RE, the fourth and fifth selected bands were extremely close to each other, i.e., 723.8 nm and 721.3 nm, respectively. Therefore, the suitable number of bands to predict the fresh weight of Chinese cabbage and to commercialize the spectral imaging sensor were four bands: green (559.6 nm), red edge (768.8 nm), green (590.9 nm), and red edge (723.8 nm). The precision and accuracy of the model using four bands were almost similar to those of the model using five bands, with 0.891 for R^2, 616 g/plant for the RMSE, and 35.3% for the RE. The model with four spectral bands is considered to be better than the model with five spectral bands because it is advantageous in terms of the price reduction of the multispectral imaging sensor, and improved the processing time by the low-dimensional spectral bands. Moreover, the performance of the four-band model was similar to the PLSR model, with all of the 519 bands compared in terms of precision and accuracy, as shown in table 4 and table 5.

Figure 7 (a), developed using two spectral bands, shows low sensitivity in the high fresh weight along with the results of the models using multispectral images.

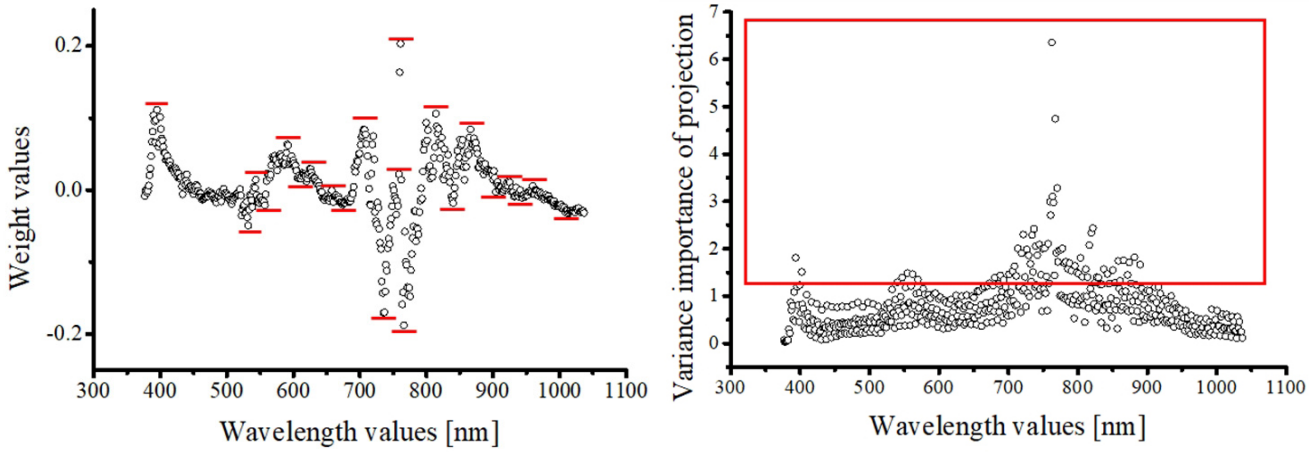

Figure 6. Reduction of high-dimensional spectral bands by weight values and variance importance in projection based on PLSR model

Table 5. Forward stepwise MLR model for predicting the fresh weight of Chinese cabbage using 98 selected bands of 519 bands

Selected Spectral bands [nm]	Equation	R^2	RMSE [g/plant]	RE [%]
559.6, 768.8	$1733.2x_1$-$6078.0x_2$+1121.2	0.741	931.8	53.5
559.6, 768.8, 590.9	$33179x_1$+$2139.7x_2$-$29071x_3$-1579.7	0.856	700.8	40.2
559.6, 768.8, 590.9, 723.8	-$9483.5x_1$+$34542x_2$+$5077.3x_3$-$15803x_{14}$-2691.1	0.891	616.0	35.3
559.6, 768.8, 590.9, 723.8, 721.3	$3151.3x_1$-$13809x_2$+$39744x_3$+$5932.3x_4$-$18273x_5$-3271.4	0.898	602.0	34.5

Reflectance values in x_1, 559.6 nm; x_2, 768.8 nm; x_3, 590.9 nm; x_4, 723.8 nm; x_5, 721.3 nm

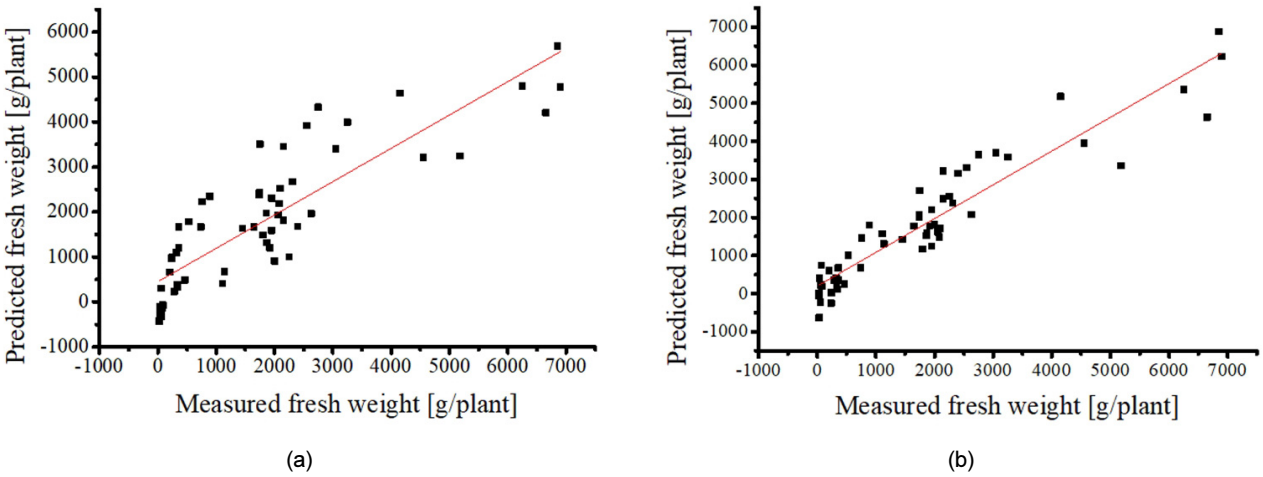

Figure 7. MLR model graph for predicting fresh weight using two spectral bands (559.60 nm and 768.77 nm) (a), using four spectral bands (559.60 nm, 768.77 nm, 590.86 nm, and 723.83 nm) (b)

Figure 7 (b), developed using four spectral bands, shows high sensitivity in the high fresh weight along with the PLSR model using all spectral bands.

Conclusions

In this research, SLR and forward stepwise MLR models with various VIs based on the reflectance of multispectral bands, and PLSR models and forward stepwise MLR models with the selected spectral bands based on the reflectance of hyperspectral bands were established and compared to predict the fresh weight of Chinese cabbage. The performance of selected spectral bands with forward stepwise MLR models was similar to that of PLSR models despite the difference in the number of selected bands. The suitable number of bands for commercializing the spectral imaging sensor were four bands: green (559.6 nm), red edge (768.8 nm), green (590.9 nm), and red edge (723.8 nm) because the fourth and fifth selected bands were extremely close to each other. The performance of the selected four bands with the forward stepwise MLR model were 0.891 for R^2, 616 g/plant for the RMSE, and 35.3% for the RE; further, no significant difference was shown when compared with the PLSR model with 0.898 for R^2, 602 g/plant for the RMSE, and 34.5% for the RE.

These results show better model performances and significant spectral bands in predicting the growth using high-dimensional data and stepwise MLR over the previous model performance developed using low-dimensional data and SLR of Kang et al. (2017). The MLR model is necessary to verify the integration possibility of the annual models developed in other years using the growth environment information to be adapted to various environmental conditions (Ryu et al., 2011).

Many issues that need to be improved to produce a commercial imaging sensor. It might be necessary to select the suitable bandpass filters with FWHM to commercialize the multispectral imaging sensor because the four selected bands with forward stepwise MLR model was established using the 2.8 nm bandwidth. Moreover, the precision and accuracy of the model modified with commercialized bandpass filter with FWHM were also compared with those of the four selected bands with forward stepwise MLR model. It is also necessary to accumulate the fresh weight of Chinese cabbage with several types of spectral bands to improve the performance of the models. Finally, it is necessary to verify the performance of the modified model and the commercialized spectral imaging sensor using various parameters, such as species, management, and environment.

Conflict of Interest

The authors have no conflicting financial or other interests.

Acknowledgement

This work was performed with the support of the "Advanced Production Technology Development Project" (Project title: Development of a UAV-based remote sensing technology for monitoring the growth of major upland crops, Project No.: 315011-03-3-HD020), Korea Institute of Planning and Evaluation for Technology of Food, Agriculture, Forestry and Fisheries (IPET), and Ministry of Agriculture, Food, and Rural Affairs (MAFRA).

References

Elarab, M., A. M. Ticlavilca, A. F. Torres-Rua, I. Maslova and M. McKee. 2015. Estimating chlorophyll with thermal and broadband multispectral high resolution imagery from an unmanned aerial system using relevance vector machines for precision agriculture. International Journal of Applied Earth Observation and Geoinformation 43:32-42. https://doi.org/10.1016/j.jag.2015.03.017

Gabriel, J. L., P. J. Zarco-Tejada, P. J. López-Herrera, E. Pérez-Martín, M. Alonso-Ayuso and M. Quemada. 2017. Airborne and ground level sensors for monitoring nitrogen status in a maize crop. Biosystems Engineering 160:124-133. https://doi.org/10.1016/j.biosystemseng.2017.06.003

Gitelson, A. A., Y. J. Kaufman and M. N. Merzlyak. 1996. Use of a green channel in remote sensing of global vegetation from EOS-MODIS. Remote Sensing of Environment 58(3):289-298. https://doi.org/10.1016/s0034-4257(96)00072-7

Haboudane, D., J. R. Miller, E. Pattey, P. J. Zarco-Tejada and I. B. Strachan. 2004. Hyperspectral vegetation indices and novel algorithms for predicting green LAI of crop canopies: Modeling and validation in the context of precision agriculture. Remote Sensing of Environment 90(3):337-352. https://doi.org/10.1016/j.rse.2003.12.013

Huang, Y., S. J. Thomson, H. J. Brand and K. N. Reddy. 2016. Development and evaluation of low-altitude remote sensing systems for crop production management. International Journal of Agricultural and Biological Engineering 9(4):1-11. https://doi.org/10.3965/j.ijabe.20160904.2010

Jin, X., L. Kumar, Z. Li, H. Feng, X. Xu, G. Yang and J. Wang. 2018. A review of data assimilation of remote sensing and crop models. European Journal of Agronomy 92:141-152. https://doi.org/10.1016/j.eja.2017.11.002

Jordan, C. F. 1969. Derivation of leaf-area index from quality of light on the forest floor. Ecology 50(4):663-666. https://doi.org/10.2307/1936256

Kang, Y. S., S. H. Kim, J. G. Kang, Y. K. Hong, T. K. Sarkar and C. S. Ryu. 2016. Estimation of leaf dry mass and nitrogen content for soybean using multi-spectral camera mounted on unmanned aerial vehicle. Journal of Agriculture & Life Science 50(6):183-190. https://doi.org/10.14397/jals.2016.50.6.183

Kang, Y. S., S. H. Kim, J. G. Kang, T. K. Sarkar, Y. S. Kwon, S. R. Jun and C. S. Ryu. 2017. Model assessment multi-temporal monitoring of Chinese cabbage growth using low altitude remote sensing system. Journal of Agriculture & Life Science 51(4):149-160. https://doi.org/10.14397/jals.2017.51.4.149

Li, B., J. Morris and E. B. Martin. 2002. Model selection for partial least squares regression. Chemometrics and Intelligent Laboratory Systems 64(1):79-89. https://doi.org/10.1016/S0169-7439(02)00051-5

Liu, X., K. Zhang, Z. Zhang, Q. Cao, Z. Lv, Z. Yuan, Y. Tian, W. Cao and Y. Zhu. 2017. Canopy chlorophyll density based index for estimating nitrogen status and predicting grain yield in rice. Frontiers in Plant Science 8:1829. https://doi.org/10.3389/fpls.2017.01829

Martínez, J. L., H. Saulo, H. B. Escobar and J. Leao. 2017. A new model selection criterion for partial least squares regression. Chemometrics and Intelligent Laboratory Systems 169:64-78. https://doi.org/10.1016/j.chemolab.2017.08.006

Mengmeng, D., N. Noboru, I. Atsushi and S. Yukinori. 2017. Multi-temporal monitoring of wheat growth by using images from satellite and unmanned aerial vehicle. International Journal of Agricultural and Biological Engineering 10(5):1-13. https://doi.org/10.25165/j.ijabe.20171005.3180

Mulla, D. J. 2013. Twenty-five years of remote sensing in precision agriculture: Key advances and remaining knowledge gaps. Biosystems Engineering 114(4): 358-371. https://doi.org/10.1016/j.biosystemseng.2012.08.009

Nguy-Robertson, A., A. Gitelson, Y. Peng, A. Viña, T. Arkebauer and D. Rundquist. 2012. Green leaf area index estimation in maize and soybean: Combining

vegetation indices to achieve maximal sensitivity. Agronomy Journal 104(5):1336-1347. https://doi.org/10.2134/agronj2012.0065

Noack, P. O. 2016. Estimating triticale dry matter yield in parcel plot trials from aerial and ground based spectral measurements. In: *IFAC-PapersOnLine*, pp.404-408, Laxenburg, Austria. https://doi.org/10.1016/j.ifacol.2016.10.074

Onoyama, H., C. Ryu, M. Suguri and M. Iida. 2013. Potential of hyperspectral imaging for constructing a year-invariant model to estimate the nitrogen content of rice plants at the panicle initiation stage. In: *IFAC Proceedings Volumes*, pp.219-224, Laxenburg, Austria. https://doi.org/10.3182/20130828-2-SF-3019.00054

Rouse Jr, J., R. H. Haas, J. A. Schell and D. W. Deering. 1974. Monitoring vegetation systems in the Great Plains with ERTS. Goddard Space Flight Center, Greenbelt. Washington, D.C.: GPO.

Ryu, C., M. Suguri and M. Umeda. 2011. Multivariate analysis of nitrogen content for rice at the heading stage using reflectance of airborne hyperspectral remote sensing. Field Crops Research 122(3):214-224. https://doi.org/10.1016/j.fcr.2011.03.013

Ryu, C., M. Suguri, M. Iida, M. Umeda and C. Lee. 2011. Integrating remote sensing and GIS for prediction of rice protein contents. Precision Agriculture 12(3): 378-394. https://doi.org/10.1007/s11119-010-9179-0

Sharma, L. K., H. Bu, A. Denton and D. W. Franzen. 2015. Active-optical sensors using red NDVI compared to red edge NDVI for prediction of corn grain yield in North Dakota, USA. Sensors 15(11):27832-27853. https://doi.org/10.3390/s151127832

Song, S., W. Gong, B. Zhu and X. Huang. 2011. Wavelength selection and spectral discrimination for paddy rice, with laboratory measurements of hyperspectral leaf reflectance. ISPRS Journal of Photogrammetry and Remote Sensing 66(5):672-682. https://doi.org/10.1016/j.isprsjprs.2011.05.002

Stellacci, A. M., A. Castrignanò, A. Troccoli, B. Basso and G. Buttafuoco. 2016. Selecting optimal hyperspectral bands to discriminate nitrogen status in durum wheat: a comparison of statistical approaches. Environmental Monitoring and Assessment 188(3):199. https://doi.org/10.1007/s10661-016-5171-0

Swain, K. C., S. J. Thomson and H. P. W. Jayasuriya. 2010. Adoption of an unmanned helicopter for low-altitude remote sensing to estimate yield and total biomass of a rice crop. Transactions of the ASABE *53*(1):21-27. https://doi.org/10.13031/2013.29493

Teoh, C. C., N. Mohd Nadzim, M. J. Mohd Shahmihaizan, I. Mohd Khairil Izani, K. Faizal and H. B. Mohd Shukry. 2016. Rice yield estimation using below cloud remote sensing images acquired by unmanned airborne vehicle system. International Journal on Advanced Science. Engineering and Information Technology 6(4):516-519. http://dx.doi.org/10.18517/ijaseit.6.4.898

Viña, A., A. A. Gitelson, A. L. Nguy-Robertson and Y. Peng. 2011. Comparison of different vegetation indices for the remote assessment of green leaf area index of crops. Remote Sensing of Environment 115(12):3468-3478. https://doi.org/10.1016/j.rse.2011.08.010

Wang, Y. P., K. W. Chang, R. K. Chen, J. C. Lo and Y. Shen. 2010. Large-area rice yield forecasting using satellite imageries. International Journal of Applied Earth Observation and Geoinformation 12(1):27-35. https://doi.org/10.1016/j.jag.2009.09.009

Xuefeng, L., L. Qiang, H. Shaolan, Y. Shilai, H. Deyu, W. Zhitao, X. Rangjin, Z. Yongqiang and D. Lie. 2016. Estimation of carbon and nitrogen contents in citrus canopy by low-altitude remote sensing. International Journal of Agricultural and Biological Engineering 9(5):149-157. https://doi.org/10.3965/j.ijabe.20160905.2246

Zarco-Tejada, P. J., M. L. Guillén-Climent, R. Hernández-Clemente, A. Catalina, M. R. González and P. Martín. 2013. Estimating leaf carotenoid content in vineyards using high resolution hyperspectral imagery acquired from an unmanned aerial vehicle (UAV). Agricultural and Forest Meteorology 171-172:281-294. https://doi.org/10.1016/j.agrformet.2012.12.013

Zhou, X., H. B. Zheng, X. Q. Xu, J. Y. He, X. K. Ge, X. Yao, T. Cheng, Y. Zhu, W. X. Cao and Y. C. Tian. 2017. Predicting grain yield in rice using multi-temporal vegetation indices from UAV-based multispectral and digital imagery. ISPRS Journal of Photogrammetry and Remote Sensing 130:246-255. https://doi.org/10.1016/j.isprsjprs.2017.05.003